INITIAL RELIABILITY ASSESSMENT OF A COMMERCIAL-OFF-THE-SHELF GPS SENSOR FOR GENERIC UAVS

Thanaraj T., Kailun Tan, C. H. John Wang, and Ee Meng Ng
Air Traffic Management Research Institute, Nanyang Technological University Singapore
Kin Huat Low, School of Mechanical and Aerospace Engineering,
Nanyang Technological University Singapore

Abstract

Unmanned aerial vehicles (UAVs) have gathered much attention commercially in recent times owing to the advancement in technology, such as the introduction of brushless-DC motors and micro-electromechanical systems (MEMS). As a result, these UAVs can undertake complex missions and pose potential benefits to a multitude of use cases, for instance, last-mile cargo delivery, infrastructure inspection, and even search-and-rescue missions. With the increase in the adoption of UAVs and the abundance of commercial-off-the-shelf (COTS) components, the airworthiness of the UAVs grows to be of concern as the assessment criteria for them are not as stringent as that of manned aircraft, largely due to the absence of an onboard pilot or passengers. In addition, UAVs with COTS components lack data to provide assurance of their reliability and determine if the UAVs are fit to fly. On-board navigational sensors are one of the critical subsystems in a UAV and any deterioration in the performance of these sensors can precipitate into a UAV system failure during flight missions, potentially leading to a crash. As such, the reliability of these sensors has to be ascertained before any flight mission to ensure their airworthiness. In this paper, we will assess a COTS GPS sensor that has been commonly used in self-assembled UAVs and predict its reliability based on the characteristics of the Surface Mounted Devices (SMD) and Integrated Circuits (IC) using MIL-HDBK-217F. Results from this assessment will provide a preliminary representation of the reliability of a typical COTS GPS sensor for the determination of its suitability for its intended operation.

Introduction

With increasing interest in introducing Unmanned Aerial Vehicles (UAV), especially ones with multirotor configuration, into urban airspace for delivery and passenger-carrying services, it has become more important than ever to assess the risk and safety aspect of UAV operation as a part of Unmanned Aircraft System (UAS) Traffic Management (UTM). While the Joint Authorities for Rulemaking of Unmanned Systems (JARUS) has published a risk-assessment framework for risk assessment for specific UAS operations (SORA), much of the assessments were qualitative in nature and lacks details needed for implementation in an urban environment [1]. Some of the considerations for ground risk evaluation could include the UAS failure rate, the probability of failing UAS crashing into people, and the probability of fatality as a result of the crash [2]. The evaluation of the ground risk is fundamental to the running of UTM regardless of the UAS traffic is segregated from or integrated with the national airspace. In fact, the evaluation of UAS airworthiness and reliability against its relationship to ground-risk informed UAS failure threshold makes up the first step of operation approval flow in the ATMRI UTM road-map (Figure 1) for increasing UTM complexity: starting with segregated visual line of sight (VLoS) operations on the left, pre-flight separation assurance to support VLoS and BVLoS operations, and finally cooperative UTM with real-time (en-route) monitoring, risk profile update, and tactical (networked) separation assurance.

As there is currently insufficient flight and accidents data from UAS operations being reported and made publicly available, the fault-tree analysis approach would be needed to estimate the UAS failure rate for ground risk evaluation. The fault tree for generic hobbyist grade quadrotor could be further divided into single point of failure and multi-point of failure faults. The former includes a motor or propeller where a single point of failure could bring down the multirotor, while the latter applies to crashes where multiple component failures must be experienced, e.g. C2 link and GNSS receiver. This paper documents the process of evaluating the failure rate of the GNSS

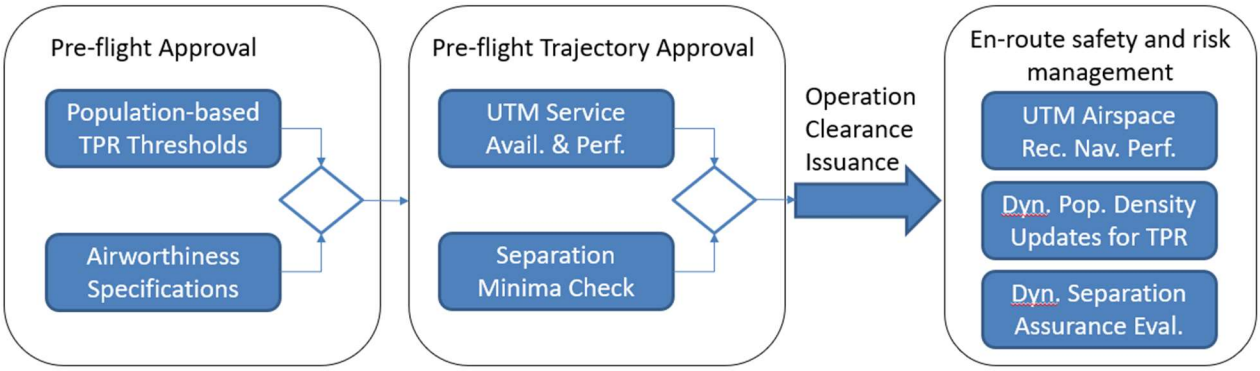

Figure 1. ATMRI's UTM Operation Flow Chart

receiver/GPS sensor to support the failure rate analysis for a generic quadrotor.

Literature Review

Risk management has always been a part of air traffic management. It also plays an important role in shaping the upcoming development of UAS traffic management, as highlighted in the various Concept of Operations (ConOps) published by the aviation authorities and affiliated research organizations [3], [4]. Due to the risk associated with the UAS traffic, the ConOps generally only allows unrestricted UAS operation away from other airspace users unless the UAS were able to meet and adhere to the standards governing civil aviation aircraft as in the case of Remote Piloted Aircraft Systems (RPAS) [5]; for operations over a populated area, the ground risk class from SORA framework is often cited but provide little guidance on quantitative evaluation of the risk involved[1] [1], [3].

Ground Risk Analysis Framework

Given the importance of ground risk evaluation for UAS operation over population centers, however, various ground risk evaluation methods have been proposed analyses. Most ground risk analysis shared similar high-level formulation, involving factors such as the probability of failure, the probability of failed UAS crashing into any ground population, and the probability of such crash resulting in a fatality. For the UAS operation to be considered safe, the product of all the aforementioned factors must remain under a target level of safety (TLS/TLOS) that is deemed acceptable to those affected. For civil aviation and RPAS operating in shared airspace with civil aviation, the TLOS for individual systems were set at 1×10^{-9} failure/hrs (extremely improbable) for catastrophic failures, ones that resulted in fatality [6]. Such TLOS has not been well defined for UTM operation [1], [3], [7] with some arguing that using a collective risk value, a function of UAS failure rate and the number of operations in the airspace, is more suitable for urban UTM [2].

Of the three components involved in the ground risk analysis, the probability of UAS failure is the least well understood, at least for small multirotor. This is likely due to the low price point and lack of relevant manufacturing and quality assurance standards and will be expended on in the literature review. In contrast, the probability of fatality resulting from collisions with UAS of various weight classes was one of the earliest factors that were studied [8], [9], and eventually led to the establishment of a 250 g limit for multirotor operation in an urban environment without the need for registration with little restriction outside of selected airspace. Finally, the probability of a UAS crashing into someone on the ground could be evaluated by finding the overlap between the probabilistic distribution of the UAS debris and the probabilistic distribution of the ground population. The former could be estimated using various crash debris distribution models [10]–[13] to include impact scenarios such as bouncing, splattering, explosion, loose propeller blade, etc. On the other hand, the

[1] SORA Annex F for ground risk evaluation is currently under internal review and not publicly available.

probabilistic distribution of ground population could be estimated using the area's population density by assuming uniform distribution or by adapting population movement models [14].

UAS Failure Rate and Reliability

One of the more difficult factors to quantify in the ground risk analysis is the UAS failure rate for small multirotor UAS. This is in contrast to larger UAS that were designed to carry passengers or heavy cargo, where the manufacturers often adopt a reliability target of 1×10^{-9} fatality/flight hours [15], or RPAS type UAS where the airworthiness requirements and maintenance quality for civil aviation aircraft would need to be met [5]. One method for demonstrating initial and continued airworthiness compliance, part of which includes the failure rate analysis, is through safety assessment using techniques including functional hazard analysis, system safety assessment, fault tree analysis, etc. [16]–[18]

For a novel and experimental aircraft type with no existing airworthiness requirements, such as multirotor UASs, one of the common methods used to evaluate reliability is the use of fault-tree analysis [19]–[21]. This would involve the creation of a fault tree for the UAS by identifying possible failure or sequence of failures that would lead to a crash event: for example, single motor failure in multirotor UAS is generally non-recoverable without fault diagnosis algorithms [22] or specialized flight control software [23], while failure in a radio receiver would not result in a crash without the flight controller also failing. However, the task of performing fault tree analysis for small multirotor UAS is made challenging compared to the same analysis for civil aviation due to the lack of published failure rate data for the components involved.

Some of the contributing factors to this lack in failure rate data could include: lack of quality standards for existing technologies under aviation environment; lack of manufacturing standards for component manufacturers entering the low-cost market for small multirotor UAS; the lower cost of components and operation restrictions for small UAS incentivized replacement of vehicle over maintenance. Fortunately, with the increasing demand for small UAS to perform commercial operations over a wider range of airspace, there has been a push for manufacturers to supply documentation on the reliability of the UAS, e.g. the draft of ISO standards requiring manufacturers to include the mean time between failures (MTBF) for safety-critical components in future documentation [24].

Methodology

The survey of existing ConOps and standard documents contributes little to the understanding of the failure rate for small UAS. The results in the need to generate a fault tree. Instead, a detailed inspection of the components on the GPS receiver board would be needed to estimate the failure rate using MIL-HDBK-217F [25] as well as updated values from MIL-HDBK-217F Notice 2. The use of MIL-HDBK-217F was chosen instead of the more up-to-date ANSI/VITA 51.1 or Telcordia SR-332 due to its public availability. However, while planned updates to the handbook have been in the work since the early 2000s, the planned revisions G and H [26] were not publicly available as of the writing of this paper.

The reliability estimation method that was used to create the handbook, as well as another table-based reliability model, was developed with the assumption of constant failure rate using an empirical model to account for contributions by environmental factors. While the failure rate model was derived from field test data, the handbook approach was often criticized for not considering the physics of failure. The handbook approach also showed weakness in light of rapid development in technologies for microelectronics, often publishing reliability models after the technology has become obsolete and unable to provide guidance on parts produced with the latest advancement in technology [27], [28].

For this study, the baseline reliability of components not available in MIL-HDBK-217F would be estimated using numbers reported under other reliability standards, e.g. RS-332 for integrated circuit (IC) chips, reliability reported for a similar product, e.g. ceramic patch antenna, or test regime performed to certify the component, e.g. AEC-Q100 for u-Blox NEO-M8N GPS receiver module. The following section will present an overview of the fault tree for small UAS and the estimation of the failure rate for the GPS sensor.

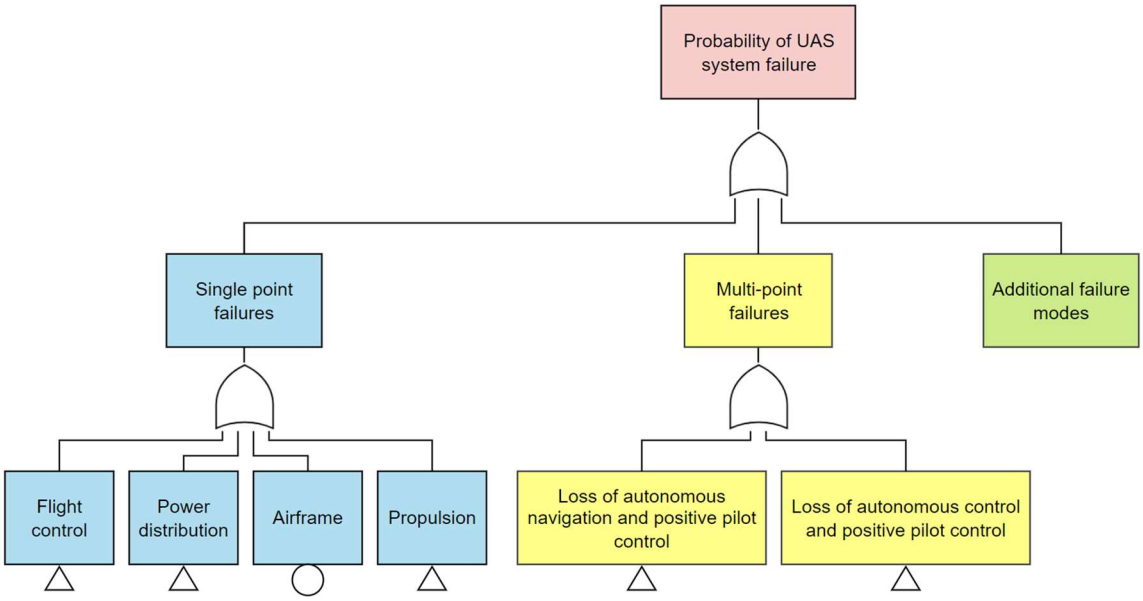

Figure 2. Fault-Tree constructed by ATMRI for a Hobbyist-Grade Quadrotor

Fault Tree Analysis for Small UAS

Fault tree analysis is an analytical and deductive approach that uses a top-level undesired event to determine its various causal events. In the context of a small UAS, the primary event in the fault tree is a system failure whereas its secondary layer of nodes describes subsystem or component failures [29]. Note that, these secondary events represent a complete failure of the subsystems or components instead of a partial failure and assumed that the UAS is irrecoverable following the system failure.

The fault tree described in Figure 2 highlights the significant events that contribute to a UAS failure, and these events are divided into single point and multiple point failures. These events are assessed to be realistic and significant in importance to an autonomous flight operation performed by a hobbyist-grade quadrotor with components: Tarot Ironman 650 airframe, PX4 Hex Cube Black flight controller, and Holybro M8N GPS receiver. These events are also assessed to be significant enough to directly lead to the top-level event, and this list is non-exhaustive and could include additional failure modes.

The single point failures consider casual events, such as flight control, power distribution, airframe, and propulsion failures, which are flight critical and a failure of one is sufficient to precipitate into a system failure. For instance, failure in the propulsion system can lead to a loss of control and eventually, lead to an uncontrolled crash.

On the other hand, multi-point failures are events that occur when two or more component failures occur at the same time. The multi-point failures presented in Figure 2 involve control and command (C2) link loss together with either the failure in autonomous navigation or failure in the autonomous flight controller. The former involves a scenario when the UAS loses access to navigational data and the latter involves the scenario when the UAS loses access to controller signals.

When the event with autonomous navigation loss and positive pilot control loss is further developed, the fault tree will consider the flight modes in which the UAS flight operation is being flown. The pilot can choose from three modes: position, altitude, or manual mode. Position mode is when the UAS can hold its position in the three-dimensional space, altitude mode is when the UAS can hold its altitude, whereas manual mode is when the pilot has full manual control over the UAS. The resulting fault tree is presented in Figure 3.

In Figure 3, the top-level event branches out to events (ANPC1, ANPC2, and ANPC3) where the

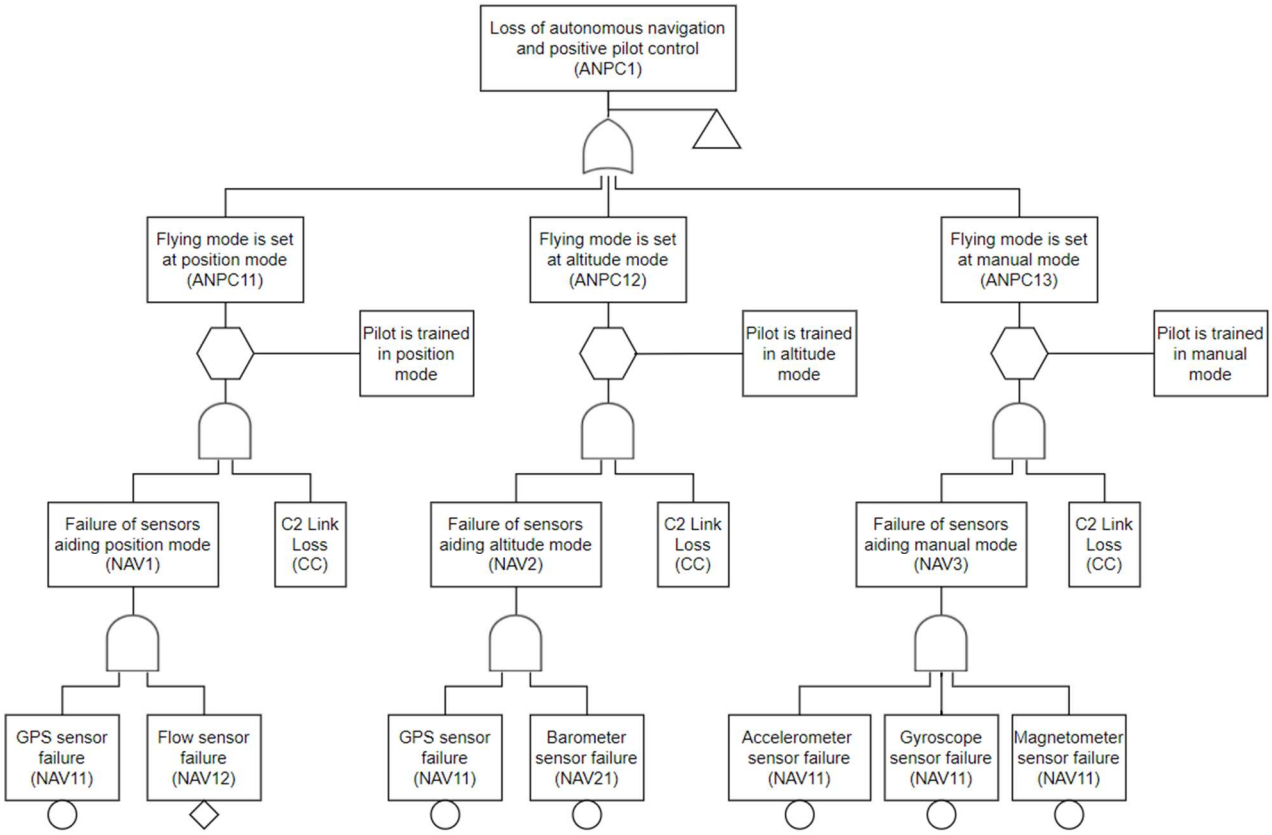

Figure 3. Fault Tree for Secondary Event (Loss of Autonomous Navigation and Positive Pilot Control).

flying operation uses three modes. Each of these events has an inhibit gate to ensure the pilot is trained in the corresponding flying mode. Following that, the events when sensors aiding the flying mode fail are considered (NAV1, NAV2, and NAV3). This event has to occur concurrently with a C2 link loss to initiate UAS system failure.

For sensor failure events, only the significant sensors that provide the source of information for the autonomous controller to perform the selected mode are considered for casual events. For position mode, GPS sensor and flow sensor are critical whereas for altitude mode, GPS and barometer sensors are important. For manual mode, since there is closed-loop feedback, the gyroscope, accelerometer, and magnetometer provide critical information to the pilot. Note that, since GPS sensor is considered in two out of the three sensors failure scenarios, it is considered important.

Studies have considered the use of fault tree analysis for UAS systems and GPS sensors have been one of the casual events [30], [31]. However, in these studies top-level events are hardware, such as ADS-B, that large UAS are generally equipped with, contrary to small UAS being considered in this paper. Also, the failure rates of the GPS module or antenna considered in these studies might not apply to small UAS. As such, we considered each component inside the GPS sensors and their associated failure rate before assessing the GPS sensor.

Component Reliability Estimation

The methodologies used in MIL-HDBK-217F with supplementary data use either the RS-332 part count method or part stress analysis method for the more recent components. The reliability data might be substituted by a component of equivalent price-point if no MTTF/FITS data are available from the manufacturer.

For microelectronic parts, the reliability prediction generally follows the equation below:

$$\lambda_P = \lambda_b \pi_T \pi_S \pi_C \pi_Q \pi_E \quad (1)$$

where λ_P is the part failure rate, λ_b is the baseline failure rate, π_T is the temperature stress factor, π_S is the electrical stress factor, π_C is the construction

(a) Front

(b) Back

Figure 4. Integrated Circuit Board for the Holybro M8N GPS Receiver showing the different components on the board.

factor, π_Q is the quality factor, and π_E is the environmental factor. Note that the value for the factors listed are empirical and presented in table form specific to the parts. For simplicity, in this analysis for application on small multirotor UAS $\pi_{T,S,C,Q}$ were all assumed as unity. π_E values were obtained from the part-specific table under the "Airborne, Rotary Wing" environment.

For more complex microcircuit components, a combined die-package failure rate equation might be used:

$$\lambda_P = (\lambda_{C1}\pi_T + \lambda_{C2}\pi_E)\pi_Q\pi_L \qquad (2)$$

where λ_{C1} is the die complexity failure rate, λ_{C2} is the package failure rate, and π_L is the manufacturing experience level ($\pi_L = 1$ for component with matured manufacturing process in place).

The baseline failure rate for specific parts could be estimated using MIL-HDBK-217F based on technology used, from manufacturer datasheet for the parts (if available[2], e.g. extracted from Ref. [32]), from datasheet of other manufacturers with parts of similar technology (e.g. data from Ref. [33]), or estimated through a known certification process that the part was put through.

An example of failure rate estimation using known certification process is for the NEO-M8N GNSS module produced by u-Blox. The module utilizes the u-Blox M8 chip, which was advertised as certified under Automotive Electronics Council's AEC-Q100 Grade 2 standard for integrated circuits. As part of the certification, 3 lots of the module with 77 samples from each lot must be subjected to a temperature of 105°C for 1000 hours or 125°C for 408 hours without showing a single failure [34]. Using the lower temperature as an example, this would mean that a total of 231 samples would survive for 1000 hours at 105°C, or a cumulative 231,000 hours without failure at this temperature.

A temperature acceleration factor, based on the Arrhenius model, could be used to estimate the failure rate at the lower temperature:

$$F_{accel} = e^{\frac{E_a}{\kappa}\left(\frac{1}{T_U}-\frac{1}{T_A}\right)} \qquad (3)$$

where F_{accel} is the acceleration factor, E_a is the activation energy (typically set at 0.7 eV for generic device), κ is the Boltzmann's constant (8.617×10^{-5} eV/K), T_U is the operational temperature in °K and T_A is the accelerated lift test temperature in °K. For the purpose of this analysis, T_U is set as 25°C or 298°K and T_A is set as 105°C or 378°K. It could be further assumed that the AEC standards were tested under the equivalent of "Ground, Mobile" environment class, of which the π_E value is typically a factor of 2 lower than the "Airborne, Rotary Wing" environment that the UAS will operate in. Thus, the contribution of the difference in environmental factors

[2] Publicly available part datasheet often does not include reliability numbers, which is only made available to paying customers.

would be included in the final calculation by multiplying the estimated failure rate by two.

Lists of critical and non-critical components (with photo) on the main board of the GPS sensor are presented in Table 1 and Table 2, respectively, along with their baseline reliabilities. Connectors and LEDs are not included in this analysis. The count number for each critical component type is presented in Table 3 where the reliability value of the IC is estimated using Eq. 2 and is not presented.

Table 1. Critical Components on the Holybro M8N GPS Receiver Main Board and their Baseline Reliability

Component	Photo	Reliability (failure/hr)	Remarks
Thin Film Chip Resistor		5.1×10^{-10}	SR-332 §8.9.1
Ceramic Chip Capacitor		6.7×10^{-10}	MIL-HDBK-217F§ 10.10
Ceramic Chip Inductor		2.3×10^{-10}	SR-332 §8.4
Receiver Module		2.7×10^{-8}	u-Blox NEO-M8N, meets AEC Q100 Grade 2
Surface Mounted IC 1 (16 pin)		5×10^{-9} 5.6×10^{-9}	7250 010, MIL-HDBK-217F N2 §5.1, 101-1000 gates, λ_{C1} & λ_{C2}
Surface Mounted IC 1 (10-pin)		5×10^{-9} 3.4×10^{-9}	C07IA2, MIL-HDBK-217F N2 §5.1, 101-1000 gates, λ_{C1} & λ_{C2}
Transistor 1 (5-pin)		6×10^{-8}	L314, assumed as MIL-HDBK-217F §6.9
Transistor 2 (6-pin)		6×10^{-8}	Unmarked, assumed as MIL-HDBK-217F §6.9
Ceramic Patch Antenna		1×10^{-6}	From similar product [31]

Initial Reliability Analysis for COTS GPS Sensor

The COTS GPS sensor analyzed in this initial study is a Holybro M8N GPS with a 10-pin connector (SKU12012), which utilizes a u-Blox M8N GNSS receiver module with NEO form factor. The reliability analysis was conducted for the mainboard, which is shown in Figure 3 with the external plastic casing removed.

The component identification was conducted visually using an enlarged photo taken using a cellphone camera. The visual identification of the components was made more challenging by the

Table 4. Non-critical Components on the Holybro M8N GPS Receiver Main Board

Component	Photo	Remarks
Buzzer		Non-critical component
Safety Switch		Non-critical, Unable to takeoff if unavailable
Button Battery		Non-critical, cold-start if unavailable

Table 2. Number of Safety Critical Components and their respective Combined Reliability Values for Holybro M8N GPS Receiver.

Component	Part Count	Combined Reliability (failure/hr)
Resistors	14	7.14×10^{-9}
Capacitors	24	1.6×10^{-8}
Inductors	3	8.1×10^{-10}
GPS Module	1	2.7×10^{-8}
IC	2	-
Transistor	2	1.2×10^{-7}
Antenna	1	1×10^{-6}

limited information provided by the markings on the mainboard and the surface-mount-device (SMD) casing. A reference photo from an older design of Holybro M8N with clear PCB marking [35] was used to help identify the SMD component, e.g. ivory color for multi-layer ceramic capacitor and white for the multi-layer ceramic inductor. Note that there is no uniform standard that links SMD component color to component type, thus mid-identification is possible.

Additional difficulties were encountered during the analysis of the u-Blox NEO-M8N GNSS Receiver Module, which is covered by a metal shield that could not be removed without destroying the unit with available equipment. While the block diagram from the NEO-M8N manual showed additional components on the module that are attached to the M8 chip, the exact component categorization and counting could not be done with the tools available. Therefore, for this initial analysis, the reliability of the M8 chip (derived from the high-temperature life test) was used to represent the entire module.

Table 3. Reliability after subjected to Environmental Modifier for Safety Critical Components on Holybro M8N GPS receiver.

Component	Environmental Modifier	Results (failure/hr)
Resistors	63	4.5×10^{-7}
Capacitors	40	6.4×10^{-7}
Inductors	16	1.3×10^{-8}
GPS Module*	2	5.4×10^{-8}
IC	0.42/8	7.6×10^{-8}
Transistor	2*16	3.8×10^{-6}
Antenna*	16	1.6×10^{-5}
Overall Reliability		2.1×10^{-5}

The combined reliability figures are further subjected to environmental factors that correspond to the "Airborne, Rotary Wing" category in MIL-HDBK-217F Notice 2 as shown in Table 4 with the following exceptions: The reliability of IC is estimated using the die/package complexity failure rate in Eq. 2 and is presented in Table 1 and with temperature/environmental modifier in Table 4; as the GPS module reliability data was obtained through testing under "Ground, Mobile" environment a factor of 2 was used to estimate the impact of the difference in operation environment; finally, an environmental modifier is not available for the ceramic patch antenna in MIL-HDBK-217F and other standards, thus the modifier value for the transistor is used instead. For semiconductor components, the thermal modifier would need to consider junction temperature, which is assumed to be 60°C; the component was assumed to be digital MOS/VHSIC CMOS for the purpose of temperature modifier computation.

The computation showed an overall reliability of 2.1×10^{-5} failures/hr, or mean time between failure (MTBF) greater than 4.76×10^{4} hours. The estimated MTBF for this unit is slightly lower than the number reported by other manufacturers, e.g. MTBF of 3.1×10^{5} hours for SPATIAL MEMS GNSS/INS by Advanced Navigation [36]. However, the estimated reliability of the Holybro M8N GPS Sensor is significantly greater than that of the propulsion system, which was quoted as having MTBF between 30 to 40 hours for small consumer-grade multirotor UAS [37].

Conclusion

With the increase in demand for UAS to conduct operations over populated areas, the assessment of the risk imposed on the general public becomes more important with helping the aviation authorities around the work in determining if such operation falls within their respective risk appetite. Some of the primary factors to be considered when assessing the ground risks are the UAS failure rate that leads to a crash, the probability of crash resulting in impact with people, and the probability of fatality from said impact. Due to the limited data available from the manufacturers, the estimation of the UAS failure rate that leads to a crash poses a challenge. The current paper explores the methodology that could be used to estimate this figure, starting with the component failure rate estimation for the GPS sensor.

The GPS sensor in question was manufactured by Holybro for PX4 using the receiver module NEO-M8N from u-Blox. The reliability estimate for this sensor unit was conducted using a combination of MIL-HDBK-217FN2 figures and formulation with supplements from the SR-322 table, reliability data from competitor products using similar technology and of similar size or derived from qualified certification from other application scenarios. The resulting reliability estimate for the GPS sensor was determined to be 2.1×10^{-5}failures/hr, or MTBF of 4.76×10^{4} hours. The result confirmed that the reliability of this GPS sensor is several orders of magnitude greater than the reliability of mechanical components such as those in the propulsion system.

It should be noted that the reliability estimates retrieved from MIL-HDBK-217F are empirically derived based on past technologies and the conditions under which the electrical component data have been collected might not be representative of conditions faced by small UAS for civil applications. Similarly, the failure rate estimated from tests conducted for automotive applications might not properly account for the vibration stress endured by multirotor components. To produce a credible ground risk estimate for UAS operation over a populated area, a failure test regime that accounts for the stress and environmental conditions experienced by multirotor should be considered. Ultimately, some form of accelerated life test using high temperature and high-frequency vibration might be needed as part of reliability reporting for UAS manufacturers wishing to participate in urban UTM.

References

[1] JARUS Work Group 6, "JARUS Guidelines on Specific Operations Risk Assessment (SORA)," Joint Authorities for Rulemaking on Umnanned Systems, JARUS Doc 6 SORA, 2019.

[2] H. A. P. Blom, C. Jiang, W. B. A. Grimme, M. Mitici, and Y. S. Cheung, "Third party risk modelling of Unmanned Aircraft System operations, with application to parcel delivery service," *Reliability Engineering & System Safety*, vol. 214, p. 107788, Oct. 2021, doi: 10.1016/j.ress.2021.107788.

[3] CORUS Consortium, "U-Space Concept of Operations," EUROCONTROL, 2019.

[4] Office of NexGen, "Unmanned Aircraft System (UAS) Traffic Management (UTM): Concept of Operations v2.0," Federal Aviation Administration, U.S.A., 2020.

[5] International Civil Aviation Organization, "Remotely Piloted Aircraft Systems (RPAS) Concept of Operations (ConOps) for International IFR Operations," ICAO, 2020.

[6] International Civil Aviation Organization, "The Procedures for Air Navigation Services—Air Traffic Management (PANS-ATM)," ICAO, ICAO Doc 4444, 2009.

[7] R. A. Clothier and R. A. Walker, "Safety Risk Management of Unmanned Aircraft Systems," in *Handbook of Unmanned Aerial Vehicles*, K. P. Valavanis and G. J. Vachtsevanos, Eds. Dordrecht: Springer Netherlands, 2015, pp. 2229–2275. doi: 10.1007/978-90-481-9707-1_39.

[8] A. la Cour-Harbo, "Mass threshold for 'harmless' drones," *International Journal of Micro Air Vehicles*, vol. 9, no. 2, 2017, doi: 10.1177/1756829317691991.

[9] C. H. Koh *et al.*, "Experimental and Simulation Weight Threshold Study for Safe Drone Operations," presented at the 2018 AIAA Information Systems-AIAA Infotech @ Aerospace, Kissimmee, Florida, Jan. 2018. doi: 10.2514/6.2018-1725.

[10] R. M. Montgomery and J. A. Ward, "Casualty Areas from Impacting Inert Debris for People in the

Open," Research Triangle Institute, RTI/5180/60-31F, 1995.

[11] Federal Aviation Administration, "Flight Safety Analysis Handbook - Federal Aviation Administration," Federal Aviation Administration, 2011. [Online]. Available: https://www.faa.gov/about/office org/headquarters offices/ast/media/Flight_Safety_Analysis_Handbook _final_9_2011v1.pdf

[12] J. A. Ball, M. Knott, and D. Burke, "Crash Lethality Model," Naval Air Warfare Center Aircraft Division, NAWCADPAX/TR-2012/196, 2012.

[13] M. J. Harwick, J. Hall, J. W. Tatom, and R. G. Baker, "Approved Methods and Algorithms for DoD Risk-Based Explosives Siting," DoD Explosion Safety Board, DDESB TP 14 Rev 3, 2009.

[14] S. H. Kim, "Third-Party Risk Analysis of Small Unmanned Aircraft Systems Operations," *Journal of Aerospace Information Systems*, vol. 17, no. 1, p. 24, 2020, doi: 10.2514/1.I010763.

[15] Volocopter Asia Holding Pte Ltd, "The Launch of Urban Air Mobility in Singapore – A Roadmap," 2022. [Online]. Available: https://volocopter-statics.azureedge.net/content/uploads/220209_Volocopter_Singapore-Roadmap.pdf

[16] Society of Automotive Engineers, "Guidelines and Methods for Conducting the Safety Assessment Process on Civil Airborne Systems and Equipment," ARP4761, 1996.

[17] Federal Aviation Administration, "Instructions for Continued Airworthiness: Aircraft Engine High Intensity Radiated Fields (HIRF) and Lightning Protection Features," Federal Aviation Administration, U.S.A., AC 33.4-3, 2017.

[18] European Aviation Safety Agency, "Certification Specifications for Large Aeroplanes," EASA, CS-25 Amendment 3, 2007.

[19] M. S. Javadi, A. Nobakht, and A. Meskarbashee, "Fault Tree Analysis Approach in Reliability Assessment of Power Systems," *International Journal of Multidisciplinary Science and Engineering*, vol. 2, no. 6, 2011, [Online]. Available: http://www.ijmse.org/Volume2/Issue6/paper9.pdf

[20] J. Hammer, A. R. Murry, and A. Lowman, "Safety Analysis Paradigm for UAS: Development and Use of a Common Architecture and Fault Tree Model," St. Petersburg, FL, U.S.A., 2017. doi: 10.1109/DASC.2017.8102039.

[21] I. Olson and E. M. Atkins, "Qualitative Failure Analysis for a Small Quadrotor Unmanned Aircraft System," 2013. doi: 10.2514/6.2013-4761.

[22] Thanaraj T, B. F. Ng, and K. H. Low, "Preliminary Study of Actuator Fault Detection for RUAVs using Neuro-Fuzzy System," in *AIAA Scitech 2021 Forum*, 0 vols., American Institute of Aeronautics and Astronautics, 2021. doi: 10.2514/6.2021-1055.

[23] A. Lanzon, A. Freddi, and S. Longhi, "Flight Control of a Quadrotor Vehicle Subsequent to a Rotor Failure," *Journal of Guidance, Control, and Dynamics*, vol. 37, no. 2, pp. 580–591, 2014, doi: 10.2514/1.59869.

[24] ISO/TC20/SC16, "Unmanned Aircraft Systems - Part 2: UAS Components," International Organization of Standardization, 21384–2, 2021.

[25] U.S.A. Department of Defense, "Military Handbook: Reliability Prediction of Electronic Equipment," Department of Defense, U.S.A., MIL-HDBK-217F, 1991.

[26] J. G. McLeish, "Enhancing MIL-HDBK-217 reliability predictions with physics of failure methods," 2010. doi: 10.1109/RAMS.2010.5448044.

[27] M. Aten, G. Towers, C. Whitley, P. Wheeler, J. Clare, and K. Bradley, "Reliability comparison of matrix and other converter topologies," *IEEE Transactions on Aerospace and Electronic Systems*, vol. 42, no. 3, pp. 867–875, 2006, doi: 10.1109/TAES.2006.248190.

[28] E. De Francesco, R. De Francesco, and E. Petritoli, "Obsolescence of the MIL-HDBK-217: A critical review," in *2017 IEEE International Workshop on Metrology for AeroSpace (MetroAeroSpace)*, 2017, pp. 282–286. doi: 10.1109/MetroAeroSpace.2017.7999581.

[29] M. Stamatelatos, W. Vesely, J. Dugan, J. Fragola, J. Minarick, and J. Railsback, "Fault tree handbook with aerospace applications," 2002.

[30] A. Tabassum, R. Sabatini, and A. Gardi, "Probabilistic Safety Assessment for UAS Separation

Assurance and Collision Avoidance Systems," vol. 6, p. 19, Feb. 2019, doi: 10.3390/aerospace6020019.

[31] K. Snyder, W. Semke, J. Gregory, M. Wing, M. Moallemi, and J. Bruce, "UAS Surveillance Criticality," *Aviation Faculty Publications*, Dec. 2016, [Online]. Available: https://commons.und.edu/avi-fac/6

[32] Avago Technologies Ltd., "10Gb Ethernet 850nm 10GBASE-SR SFP+ Transceiver Reliability Data Sheet," Avago Technologies, AFBR-700SDZ, 2010. [Online]. Available: https://www.mouser.com/datasheet/2/678/av02-2778en-1828531.pdf

[33] CTI Antennas, "GPS Active Antenna Module with a filtered LNA," AAMP Global Ltd. [Online]. Available: https://docs.rs-online.com/c1b0/0900766b80d1ee45.pdf

[34] Automotive Electronics Council, "Failure Mechanism Based Stress Test Qualification for Integrated Circuits," Automotive Electronics Council, AEC-Q100-Rev-G, 2007.

[35] coMpletLylOsT, "Holybro GPS/Compass Replacement (NEO-M8N-0-10)." 2020. [Online]. Available: https://discuss.px4.io/uploads/default/optimized/2X/6/65fc4a6bfcefc8c1a01d7ed08eeae363b81fc36f_2_512x500.jpeg

[36] Advanced Navigation Ltd., "Advanced Navigation Brochure." 2018. [Online]. Available: https://www.unmannedsystemstechnology.com/wp-content/uploads/2018/09/Advanced-Navigation-Brochure.pdf

[37] J. Moore, "Guessing when your drone will die." 2018. [Online]. Available: https://www.aopa.org/news-and-media/all-news/2018/march/05/guessing-when-your-drone-will-die

Acknowledgements

This project is supported by the National Research Foundation, Singapore, and the Civil Aviation Authority of Singapore, under the Aviation Transformation Programme. Any opinions, findings and conclusions or recommendations expressed in this material are those of the author(s) and do not reflect the views of National Research Foundation, Singapore, and the Civil Aviation Authority of Singapore. The Ph.D. candidature scholarship provided to the first author by Nanyang Technological University through Air Traffic Management Research Institute Leader's Track is greatly appreciated. The authors would also like to thank Professor Bing Feng Ng for his support to carry out this research work.